Appl. Phys. B 77, 133–137 (2003)
DOI: 10.1007/s00340-003-1257-9

Applied Physics B
Lasers and Optics

Rapid communication

I. TERROSO[1,✉]
J.P. CARVALHO[1]
O. FRAZÃO[1]
M.B. MARQUES[3]
H.M. SALGADO[2]

All-fibre wavelength conversion based on four-wave mixing in a ring erbium-doped fibre laser

[1] INESC Porto – UOSE, Unidade de Optoelectrónica e Sistemas Electrónicos, 4169-007 Porto, Portugal
[2] FEUP – DEEC, Faculdade de Engenharia da Universidade do Porto, 4200-465 Porto, Portugal
[3] FCUP – Dep. de Física, Faculdade de Ciências da Universidade do Porto, 4169-007 Porto, Portugal

Received: 14 May 2003
Published online: 30 July 2003 •

ABSTRACT A new scheme based on four-wave mixing is presented using a ring erbium-doped fibre laser and tuneable fibre Bragg gratings that can effectively perform wavelength conversion in a wide wavelength range. An application of this wavelength-conversion architecture to optical communications is also presented.

PACS 42.65.-k; 42.65.Ky

1 Introduction

All-optical wavelength conversion (WLC) can enhance the performance of wavelength division multiplexing (WDM) optical networks, and it has been a subject of intensive studies in recent years [1, 2]. Progress in optical communications has historically succeeded in providing ever larger levels of communications capacity at continually reducing costs. To date, optical communication systems have consisted typically of point-to-point links connecting electronic switching equipment with channel rates up to $10\,\mathrm{Gbit\,s^{-1}}$. Currently, in order to route optical signals through the network, optoelectronic transponders are used that consist of a receiver, an electrical switching matrix, and a laser, in order to retransmit the signal to its destination. Although these have the benefit of allowing electrical regeneration of the signal, the speeds at which the switching can be carried out is limited by the electronics. If all-optical transparent nodes could be used the transmission rates would be increased dramatically and regeneration can still be done at periodic intervals through the network. With WDM, aggregate transmission rates have been increased to the terabit per second level, so nowadays the use of practical optical techniques for processing and routing of information is becoming of great interest. Wavelength conversion is one of the most important among these. Wavelength converters in WDM networks are important for three main reasons. First, data may enter the network at a wavelength that is not suitable for use within the network. For example, the first-generation optical networks commonly transmit data in the 1310-nm wavelength window, using LEDs or Fabry–Perot lasers. Neither the wavelength nor the type of laser is compatible with WDM networks. So, at the inputs and outputs of the network, data must be converted from these wavelengths to narrow-band WDM signals in the 1550-nm wavelength range. A wavelength converter used to perform this function is sometimes called a transponder. Second, wavelength converters may be needed within the network to improve the utilization of the available wavelengths on the network links. Finally, wavelength converters may be needed at boundaries between different networks if the different networks are managed by different entities and these entities do not coordinate the allocation of wavelengths in their networks. Several techniques have been presented for all-optical wavelength conversion, such as optoelectronic conversion, cross-gain modulation in semiconductor optical amplifiers (SOAs) [3], cross-phase modulation in SOAs [4], difference-frequency generation in semiconductor waveguides [5], and four-wave mixing [6]. Four-wave mixing (FWM) for wavelength conversion has advantages that include large spectral and dynamic range as well as providing strict bit rate and modulation format transparency. This technique can also operate at bit rates as high as $100\,\mathrm{Gbit\,s^{-1}}$ [7]. Other techniques are not transparent in terms of signal format and produce a converted signal data-inverted in relation to the input signal. Since FWM preserves both phase and amplitude information, it is a type of wavelength conversion that is strictly transparent, making it one of the most reliable wavelength-conversion processes. Here a technique based on FWM is presented to achieve flexible wavelength conversion using a ring erbium-doped fibre laser and tuneable fibre Bragg gratings over a wide range of wavelengths.

2 Theoretical treatment

2.1 *General description*

Four-wave mixing is a third-order non-linearity in silica fibres, which is analogous to intermodulation distortion in electrical systems, so that in multichannel systems three optical frequencies mix to generate a fourth:

$$f_g = f_i + f_j - f_k \tag{1}$$

(f_i, f_j, f_k are not necessarily distinct). This phenomenon is termed four-wave

✉ E-mail: iterroso@inescporto.pt

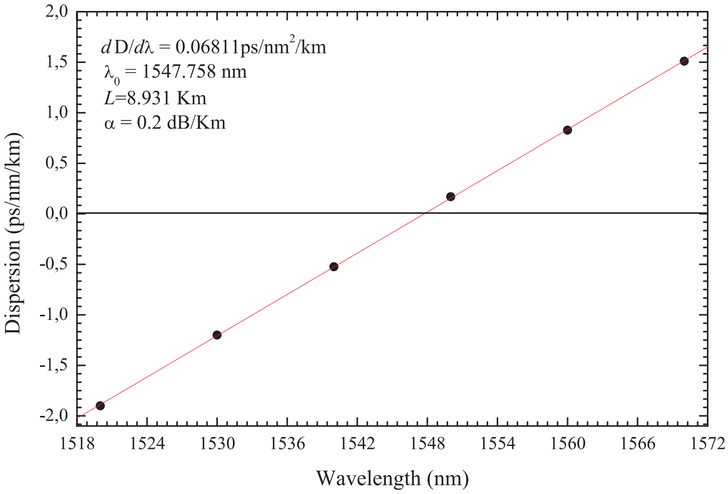

FIGURE 1 Dispersion characteristics of the dispersion-shifted fibre (DSF) used (SMF-DF Corning)

mixing. Considering that the input, continuous waves, and signals are not depleted by the generation of the mixing products, and that the states of polarization of these signals are equal and do not change along the propagation, the optical power of the new generated signal is well known and can be obtained from [8, 9]. The FWM efficiency, $\eta_{i,j,k}$, is given by

$$\eta_{i,j,k} = -\frac{\alpha^2}{\alpha^2 + \Delta\beta^2_{i,j,k}} \times \left[1 + \frac{4\,\mathrm{e}^{-\alpha L}\sin(\Delta\beta^2_{i,j,k})}{\left(1-\mathrm{e}^{-\alpha L}\right)^2}\right], \quad (2)$$

where α is the optical fibre attenuation in dB km^{-1}, L is the fibre length, and the phase mismatch, $\Delta\beta^2_{i,j,k}$, is the difference of the propagation constants of the various waves due to chromatic dispersion. When two of the three input channels are degenerate ($f_i = f_j$) the phase mismatch for a dispersion-shifted fibre around the zero-dispersion wavelength, λ_0, is given by [10]

$$\Delta\beta = -\frac{\lambda^4\pi}{c^2}\frac{\mathrm{d}D_\mathrm{c}}{\mathrm{d}\lambda} 2(f_i - f_k)^2(f_i - f_0), \quad (3)$$

where $\mathrm{d}D_\mathrm{c}/\mathrm{d}\lambda$ is the slope of the dispersion that can be evaluated in Fig. 1. The phase-matching condition is always satisfied when f_i coincides with the zero-dispersion wavelength, i.e. $f_i = f_0$.

3 Experimental work

3.1 *Description of the setup*

The setup used for this experiment is depicted in Fig. 2. This setup is composed of a ring erbium-doped fibre laser, which in turn is composed of an erbium-doped fibre amplifier (EDFA), an optical circulator (OC), and a fibre Bragg grating (FBG) which selects the lasing wavelength that gets fed back to the ring and is amplified by the EDFA forming an external cavity. The laser signal produced by this ring laser is used as a pump source for the four-wave-mixing phenomenon. Another laser beam, from a tuneable multiwavelength laser source, is introduced through an optical coupler into the ring. The polarization state of this source is maintained stable though a polarization controller to maximize the FWM process efficiency, i.e. maintaining it in a position where the largest amount of FWM power was generated. Inside the ring, a dispersion-shifted fibre (DSF) with ~ 9 km in length is placed in order to enhance the non-linear effects that lead to FWM. This fibre has a very low birefringence, an attenuation of 0.2 dB km^{-1}, and a dispersion slope of 0.06811 ps nm^{-2} km^{-1}. The zero-dispersion wavelength of this fibre is 1547.758 nm. The combination of these two signals, pump and user signal, generate a third signal, the conjugate signal. This signal is obtained directly after filtering with the FBG $\lambda_{\mathrm{B\,conjugate}}$. It is represented in Fig. 2 by inset (B).

Inside the ring, the optical power is distributed over two perpendicular states of polarization that vary along the ring. The polarized input signal then interacts and combines with the state of polarization of the pump. This leads to an average value of the FWM power

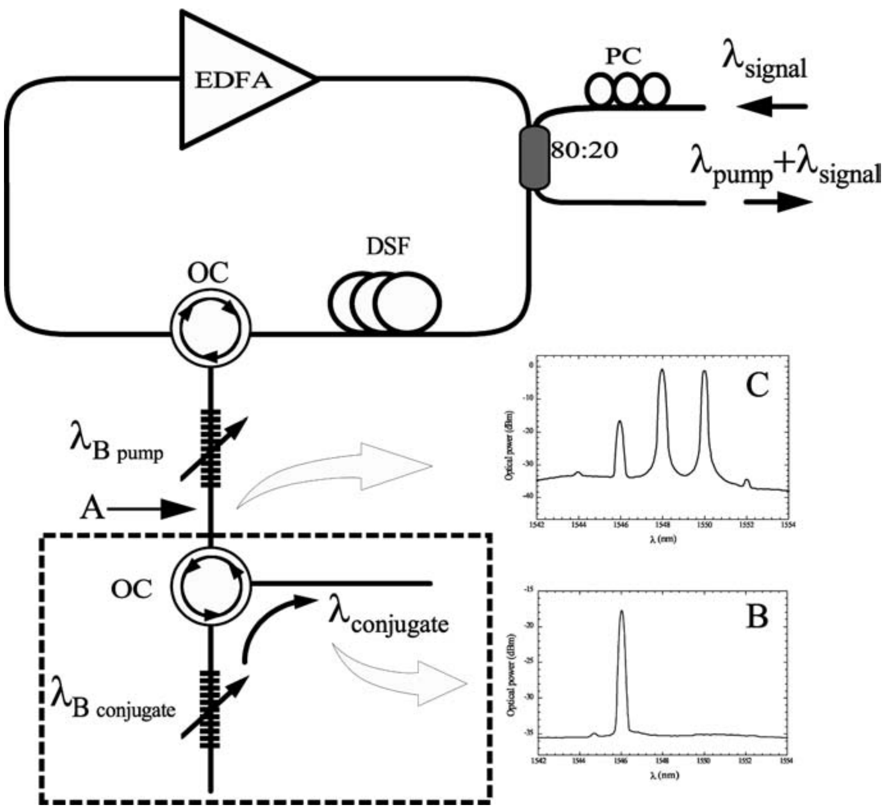

FIGURE 2 Experimental setup of the all-fibre wavelength converter

that is relatively insensitive to polarization changes of the input signal. Although these are coherent sources, they interact non-coherently inside the ring. The FWM output power could be maximized if a single polarization state was used inside the ring. This would introduce more demanding phase-matching conditions into the system and make the FWM process extremely sensitive to polarization changes. The efficiency of the FWM process is maximum (in the degenerate case) when the pump wavelength (pump) is placed at the zero-dispersion wavelength. This occurs because the group velocity of the interacting waves is less affected by chromatic dispersion at this point. This increases the phase matching and consequently increases the FWM process efficiency.

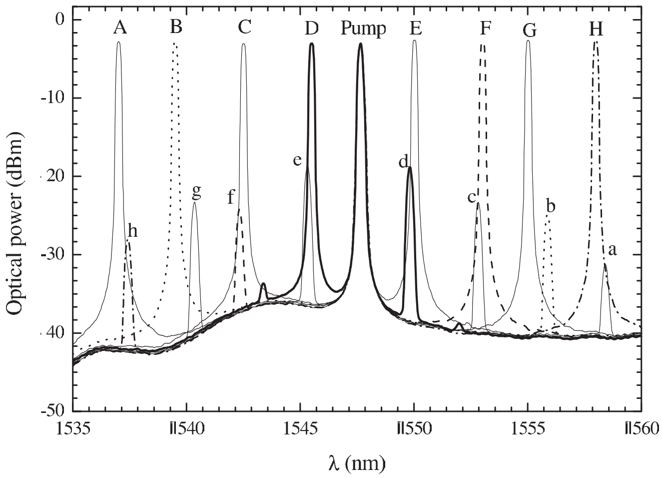

FIGURE 3 Sample of the optical spectra when λ of the input signal is changed. (A–H – input signal; a–h – corresponding converted FWM component)

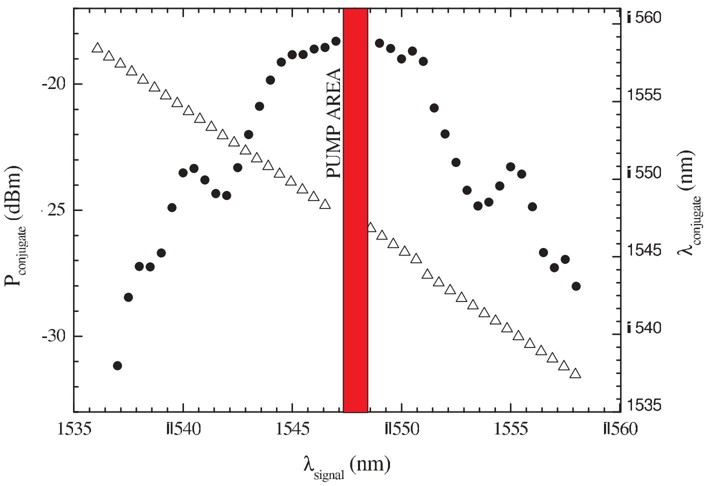

FIGURE 4 Relationship between λ of the input signal and λ and power of the resulting conjugate as λ of the input signal is changed keeping the power constant

3.2 *Experimental results*

The output of the multiwavelength distributed-feedback laser signal has an output power of approximately 10 mW (10 dB m). This signal is combined with a pump signal from the erbium-doped fibre laser with a peak power of 6.3 mW (8 dB m) through the optical coupler. Only 20% of the input signal passes through the coupler and 80% of the pump signal is continuously fed back into the ring due to the FBG ($\lambda_{\mathrm{B\,pump}}$). Inside the ring these two interacting signals generate the FWM conjugate replica of the output of the multiwavelength laser. Measurements are always taken at point (A) where we have only 10% of the pump signal power because the grating has a reflectivity of 90% and a FHWM of 0.2 nm. This does not affect the remaining signals since they are not in the spectral reflection range of the gratings.

As a first experiment the wavelength of the input laser is changed to verify the resulting change in wavelength and power of the FWM conjugate. This can be observed in Fig. 3. It can be seen that a large span can be achieved with the peak power difference between conjugates being mainly due to the efficiency of the FWM process although there is a contribution from the EDFA gain profile.

The wavelength-translation relationship between the signal and its conjugate is almost linear. These two signals maintain themselves symmetric with respect to the pump. This result can be verified in Fig. 4 where the pump has been placed at the zero-dispersion wavelength. In this figure, the peak power for each conjugate can also be seen. The shaded area in the center corresponds to the pump area where all the signals are overlapping. In this area measurements cannot be taken because the signals are not distinguishable from each other. The total variation in conjugate power is approximately 10 dB m, and a wide range of about 10 nm is achieved with relatively stable power levels.

The FWM efficiency can only be evaluated if the wavelength of the pump signal is varied in a given interval around the zero-dispersion wavelength. According to the theoretical assumptions, maximum wavelength-conversion efficiency can be obtained by placing the pump near the zero-dispersion wavelength to obtain maximum phase matching. The present configuration permits accurate variation of the pump wavelength through the application of strain to the FBG. The results of this experiment are presented in Fig. 5.

The input signal is maintained stable at 1550 nm and the pump signal is changed from 1545 nm to 1548.5 nm. It can be clearly seen that the best results are obtained when the pump signal is placed near the zero-dispersion wavelength. In fact, when the pump exactly matches the zero-dispersion wavelength, maximum output power of the converted signal is obtained, as represented by the bold solid line in Fig. 5 (curves A–a).

Figure 6 gives a clearer view of this phenomenon. Here we can see the relationship between the pump wave-

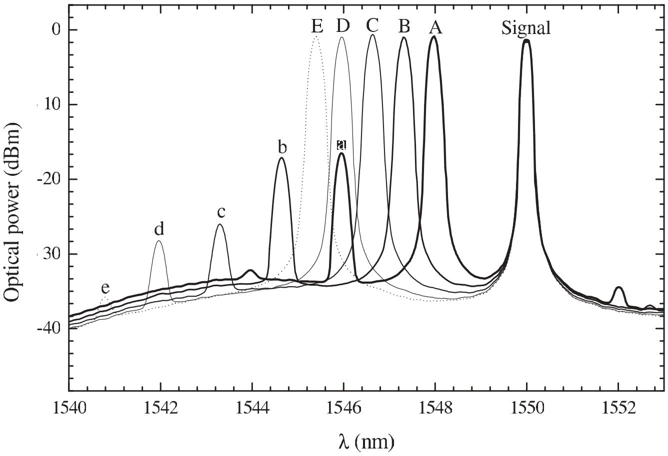

FIGURE 5 Sample of the optical spectra when λ of the pump signal is changed by the application of strain to the FBG. (A–E – pump; a–e – converted FWM component)

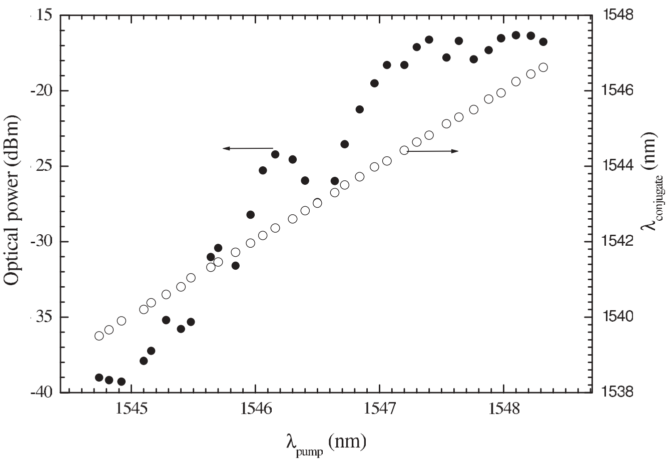

FIGURE 6 Relationship between the wavelength of the input signal and the wavelength and power of the resulting conjugate as the pump signal is changed

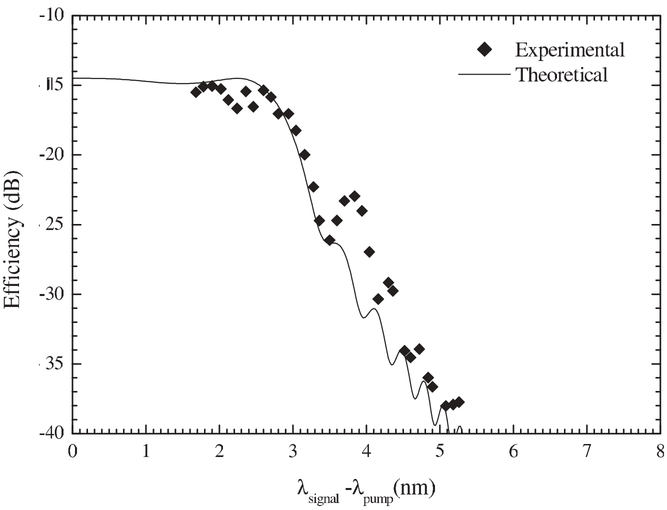

FIGURE 7 FWM efficiency dependence on separation between input signal and pump signal

length and the conjugate wavelength as well as the peak power of the FWM conjugate. It is seen that the FWM conjugate exhibits a total power variation of approximately 25 dB m over the range of 1538 nm to 1548 nm of the pump signal. Efficiency calculations lead to Fig. 7, where both the theoretical and practical efficiency results are presented.

The differences between the theoretical results and the experimental results are due to the zero-dispersion deviation along the fibre length. The use of short-length highly non-linear dispersion shifted fibre would reduce this discrepancy.

3.3 *Application to optical communications*

As mentioned earlier, the main purpose of this wavelength converter is to enhance the capabilities of wavelength-routing optical communication networks (WDMs). According to this claim we present here a possible application of this wavelength converter to an optical cross-connect (OXC) [11, 12]. This structure can be seen in Fig. 8 where we see a block diagram of an OXC that includes wavelength conversion. The inclusion of this capability in the OXC is very important because whenever we need to send the channel of the same wavelength to the same output port we can now perform wavelength conversion on one of them and avoid destructive interference between these two channels.

To ensure the ability to perform wavelength conversion, this OXC is equipped with a wavelength-conversion unit. This unit is composed of OCs, FBGs, multiplexers (MUX), demultiplexers (DEMUX), and a series of wavelength converters (WC1). The wavelength-conversion unit selects the wavelength channels that need to be converted and through reflection in a Bragg grating array (BGA) redirects them to a DEMUX [13, 14]. This splits the incoming channels to different wavelength converters that operate individually on each channel. After conversion all channels are put back together by a MUX. It should be noted that a situation where all the channels need wavelength conversion is highly improbable, so the use of a lot of wavelength converters does not become necessary, decreasing the overall cost of this solution. The architecture of each wavelength-converting unit is as described in this article.

4 Conclusions

We have demonstrated an all-fibre wavelength converter based on

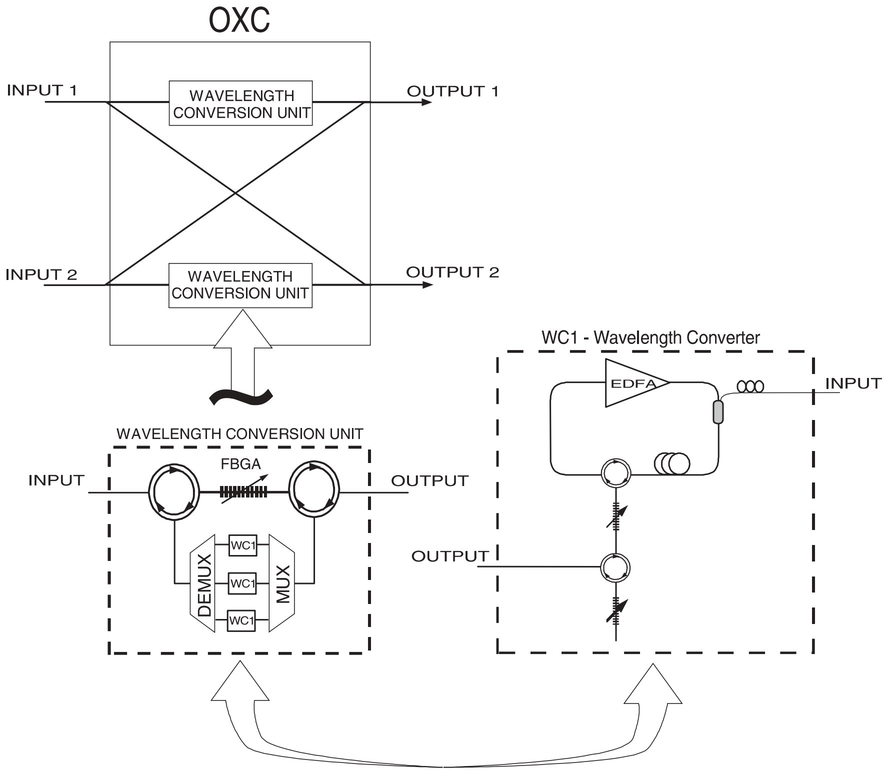

FIGURE 8 Application of the wavelength converter in optical communications

four-wave mixing in a ring erbium-doped fibre laser. Degenerate FWM near the zero dispersion wavelength region is studied. The experimental results are in good agreement with theory. Performance levels are limited by the type of fibre used (DSF), which does not have a sufficiently high nonlinear coefficient to ensure good degenerate FWM process efficiency levels. Nonetheless, the results compare favorably with previous published results. This structure is also very resistant to changes in the polarization state of the interacting signals. We are pursuing all-fibre FWM wavelength conversion because of the feasible advantage of its transparency; the conversion can be insensitive to the modulation bit rate and format, in contrast to grating-type wavelength conversion. New types of fibre are being developed every day and efficiency levels reached are getting higher, which leads us to believe this field will have great growth in the coming years. Future work will include the use of different types of fibre in this structure, like highly nonlinear dispersion-shifted fibre (HNLDSF) and photonic crystal fibre (PCF), which will enhance its capabilities by the use of smaller amounts of fibre to achieve more efficient wavelength conversion. The use of a higher number of FBGs will allow this configuration to perform non-degenerate FWM. Efficient polarization-control schemes may also be used to maximize the conversion efficiency while maintaining the whole system stable. This configuration for wavelength conversion has a pending patent application. We have also presented a possible application of this wavelength-conversion architecture to optical communications, showing its integration in the structure of an optical cross-connect (OXC). Other architectures for the wavelength-conversion unit are in current development and will be the object of future work, as well as the application of this wavelength converter to high bit rate (40 $\mathrm{Gbit\,s^{-1}}$) optical networks.

REFERENCES

1 J.M.H. Elmirghani, H.T. Mouftah: IEEE Commun. Magn. **38**, 86 (2000)
2 A. Kloch, P.B. Hansen, D. Wolfson, T. Fjelde, K. Stubkjaer: IEICE Trans. Electron. **E82-C**, 1475 (1999)
3 M.F.C. Stephens, D. Nesset, K.A. Williams, A.E. Kelly, R.V. Penty, I.H. White, M.J. Fice: Electron. Lett. **35**, 1762 (1999)
4 M. Schilling, K. Daub, W. Idler, D. Baums, U. Koerner, E. Lach, G. Laube, K. Wunsterl: Electron. Lett. **30**, 2128 (1994)
5 M.L. Bortz, D. Serkland, M.M. Fejer, S.J.B. Yoo: Near-degenerate difference frequency generation at 1.3 m in linbo3 waveguides for application as an all-optical channel shifter. In: CLEO 1994, paper CTHD6
6 K. Inoue, Hiromu Toba: IEEE Photon. Techol. Lett., **4**, 69 (1992)
7 A.E. Kelly, A.D. Ellis, D. Nesset, R. Kashyap, D.G. Moodie: Electron. Lett. **34**, 1955 (1998)
8 R.W. Tkach, A.R. Chraplyvy, F. Forghieri, A.H. Gnauck, R.M. Derosier: IEEE J. Lightwave Technol. **13**, 841 (1995)
9 K. Inoue: IEEE J. Lightwave Technol. **10**, 1553 (1992)
10 K. Inoue: IEEE J. Quantum Electron. **QE-28**, 883 (1992)
11 O. Frazão, J.P. Carvalho, I. Terroso, V. Barbosa, H.M. Salgado: 'A novel architecture of an optical cross-connect based on tuneable fibre bragg gratings and optical circulators'. In London Communications Symposium (2002) pp. 53–56
12 O. Frazão, I. Terroso, J.P. Carvalho, H.M. Salgado: Opt. Commun. **220**, 105 (2003)
13 V. Mizrahi, R. Erdogan, D.J. DiGiovanni, P.J. Lemaire, W.M. MacDonald, S.G. Kosiski, S. Cabot, J.E. Sipe: Electron. Lett. **30**, 780 (1994)
14 J.J. Pan, Y. Shi: Electron. Lett. **34**, 74 (1998)